Science & Technology Development Journal – Engineering and Technology, 5(S1):109-119

Open Access Full Text Article

Research Article

Polyimide sponge fabricated by controlled phase separation of ternary solution for heat-resistant triboelectric nanogenerator

Thu Ha Le[1,2], Ngoc Mai Chau[1,2], Thi Le Thanh Nguyen[1,2], Van Tien Bui[1,2,*]

Use your smartphone to scan this QR code and download this article

ABSTRACT

Triboelectric nanogenerator (TENG) has gained increasing attention owing to their diverse applications, especially as an indispensable power supply for rechargeable sensors and wearable portable electronic devices in the IoT era. However, dielectric materials for fabricating TENG are mostly thermoplastic polymers, which are normally unsatisfactory and easily deteriorated at elevated temperatures, thereby hindering its applications in harsh environments. In this research, customizable polyimide (PI) membranes were prepared by a facile and scalable solution phase separation for a heat-resistant high-power TENG. A mixture of *N, N*-dimethylacetamide and methanol is exploited as a proper pair of solvent and nonsolvent to induce phase separation, resulting in the formation of porous structures. The results showed that PI films possessed uniform and high porosity, and especially, they have excellent thermal stability compared to commercial thermoplastic membranes such as the Celgard. The new porous PI-based TENG device exhibited a significant enhancement in electrical output of 10 times and 2 times compared with TENGs based on flat PI and commercial Kapton, respectively. More importantly, a new antagonist-structured TENG composed of microdome-convex chitosan and porous-concave PI could generate a superior output voltage of 180 V, which could directly power a ``HCMUT'' panel with 102 light-emitting diodes (LEDs). Besides the advantages such as superior output, excellent temperature resistance and ease of scaling up, our new TENG is highly potential to be applied in specific applications such as self-powered electronic systems working in harsh environments.

Key words: Phase separation, porous structure, sponge, polyimide, triboelectric nanogenerator

[1]*Department of Polymer Materials, Polymer Research Center, Faculty of Materials Technology, Ho Chi Minh City University of Technology (HCMUT), 268 Ly Thuong Kiet Street, District 10, Ho Chi Minh City, Viet Nam*

[2]*Vietnam National University Ho Chi Minh City, Linh Trung Ward, Ho Chi Minh City, Viet Nam*

Correspondence

Van Tien Bui, Department of Polymer Materials, Polymer Research Center, Faculty of Materials Technology, Ho Chi Minh City University of Technology (HCMUT), 268 Ly Thuong Kiet Street, District 10, Ho Chi Minh City, Viet Nam

Vietnam National University Ho Chi Minh City, Linh Trung Ward, Ho Chi Minh City, Viet Nam

Email: tienbv@hcmut.edu.vn

History

- Received: 25-04-2022
- Accepted: 31-01-2023
- Published: 15-02-2023

DOI :

https://doi.org/10.32508/stdjet.v5iSI1.990

Check for updates

INTRODUCTION

With the arrival of the new era of Internet of things (IoT), wireless sensor networks (WSNs) which can gather data and wirelessly transmit that data through a network to a processing server are becoming indispensable for communication in the IoT system[1]. Since WSNs comprise a huge number of sensors, a significant rise in the number of existing IoT sensors have been recognized recently. For real-time communication in IoT, the portable and wearable sensors normally require properly electrical power sources with light-weight, flexible, self-charged and distributed characteristics which remain challenges with conventional batteries and supercapacitors[2,3]. Recently, invented by Zhong Lin Wang's group in 2012, triboelectric nanogenerators (TENGs) have become one of the most inspired technologies which can convert kinetic mechanical energy to electricity[4]. TENGs have been considered as a promising and inevitable power supply for self-charged portable wearable sensors because they possess lightweight, good flexibility, high energy conversion efficiency and environmentally friendly[5]. These characteristics normally come from the flexible thermoplastics which are usually used as tribo-dielectrics in TENG. Nevertheless, thermoplastics also suffer from big drawbacks including low mechanical strength and poor heat resistance. These obstacles obviously hinder the potential applications of TENG in harsh environments. However, unlike other plastics, polyimide (PI) exhibits exceptional advantages of thermal stability, mechanical toughness, and chemical resistance. In addition, PI has promising dielectric properties[6]. Therefore, PI was already exploited as a promising negatively charged tribo-material in TENG. However, it should be noted that PI was usually used in the form of flat film (commercially denoted as Kapton®) because the common PI polymer possesses insolubility in almost organic solvents as well as difficulty in thermal processing. It was reported that TENGs made of Kapton exhibited unsatisfactory output performance as a result of inherently poor electrification effectiveness of the flat surface of the Kapton[7,8].

It is obvious that the electric output of a TENG device must be crucially important for its practical applications. To enhance TENG output, three common ap-

Cite this article : Le T H, Chau N M, Nguyen T L T, Bui V T. **Polyimide sponge fabricated by controlled phase separation of ternary solution for heat-resistant triboelectric nanogenerator**. *Sci. Tech. Dev. J. – Engineering and Technology;* 5(S1):109-119.

proaches are usually applied including proper selection of materials[6], surface and structure engineering of electrets[9],and rational design of TENG device[10,11]. Among them, enhancing the effective contact area of dielectrics have widely used for boosting TENG performance. In the case of PI, there were several efforts for making its structural design such as PI aerogel[12,13], porous PI[14,15], etc. However, it should be noted that the existing methods remain some disadvantages including low scalability and high production cost, which constrain the commercialization of TENG in large applications. Therefore, finding a new method for massive production of PI with designed controllable structure for high-performance and robust TENG is highly desirable.

In this work, we proposed a rapid and scalable method to fabricate the porous PI by the simple solution phase separation method. A solution of PI, N, N-dimethylacetamide and methanol was used to induce phase separation through solvents evaporation. The porous structure and uniformity of the PI membrane was controlled by the ratio of DMAc/MeOH. The PI membrane then applied for a TENG, thereby TENG output performance was characterized. Moreover, the temperature-resistant ability of the PI membrane also was evaluated.

EXPERIMENTAL METHODS

Materials

Polyimide (PI) resin powder, which is dissolvable in organic solvents, was bought from Alfa Aesar (USA). Chitosan (from shrimp shells; $\geq$ 75 % (deacetylated)) was purchased from Sigma Aldrich (USA). N, N-dimethylacetamide (DMAc, 99.8%), and methanol (MeOH; 99.8 %) were purchased from Sigma-Aldrich (USA) and used as received. Acetic acid (99.5 %) was bought from Xilong (China). Copper foil (thickness of 0.5 mm) was kindly supplied by Nhat Phat Co. (Vietnam). The substrates were ultrasonically washed with acetone, diluted aqueous acid solution and distilled water successively, followed by drying under nitrogen gas before use.

Preparation of porous films

PI solution was prepared first by dissolving a predetermined amount of PI in DMAc. MeOH was then added, and the solution stirring was kept for 4 h to obtain the homogeneous yellow ternary solution containing PI and DMAc/MeOH as a solvent/nonsolvent pair. Note that the solution should be aged for 1 h before fabricating film.

For preparing PI sponge, the pre-cleaned copper substrate was dipped into the as-prepared ternary solution, followed by drying in an ambient environment (temperature of 27 °C and relative humidity of 68 %). The other dipping conditions were fixed as the withdrawal speed of 60 cm/min and the dipping time of 5 s. PI thin film with a three-dimensional (3D) interconnected porous structure was spontaneously formed on the copper surface after drying through spinodal decomposition of the PI/DMAc/MeOH ternary solution (Figure 2). The polymer concentration was adjusted to investigate the effect of these factors on porous structure of PI thin film.

Fabrication of micro-patterned Chitosan

Chitosan serves as a positively charged tribo-surface for a TENG. Chitosan film with microdome-patterned surface was fabricated via solution molding processes (Figure 1). Briefly, a polystyrene film with highly ordered honeycomb concave structure (*hc*-PS) was first prepared via the improved phase separation (IPS) method following a previous report[16] and then it was used as a master mold. Meanwhile, viscous chitosan solution (2 wt. %) was also prepared in 1 vol. % aqueous acetic acid solution.

Subsequently, chitosan solution was drop-casted onto the as-prepared *hc*-PS mold, followed by degassing processes through reduced pressure which facilitate chitosan to perfectly fill up into pores of the *hc*-PS film. The as-prepared sample was then dried in air for 4 h and in an oven at 80 °C before detaching the replica chitosan from the mold. Patterned chitosan was stored in a low-humidity desiccator before use.

Assembly of TENG device

Herein, TENG device was assembled in the most simple contact-separation working mode (C-S mode). Correspondingly, the as-prepared PI sponge on copper substrate and the patterned chitosan were used directly to fabricate the TENG device. A PI sponge serves as a negatively charged tribo-layer, while the copper substrate plays a role as a bottom electrode. The PI sponge on the copper substrate was adhered on a poly(methyl methacrylate) (PMMA) supporter by the double-sided adhesive tape. In addition, the patterned chitosan film on another PMMA supporter with a copper foil sandwiched between them was used as a counter tribo-component of the TENG. TENG devices with the same dimension of 2.5 cm $\times$ 2.5 cm were used for all electrical output characterizations. The gap between the two tribo-surfaces was fixed at about 5 mm. Finally, both the top and the bottom electrodes were connected by the electric wires for measurement.

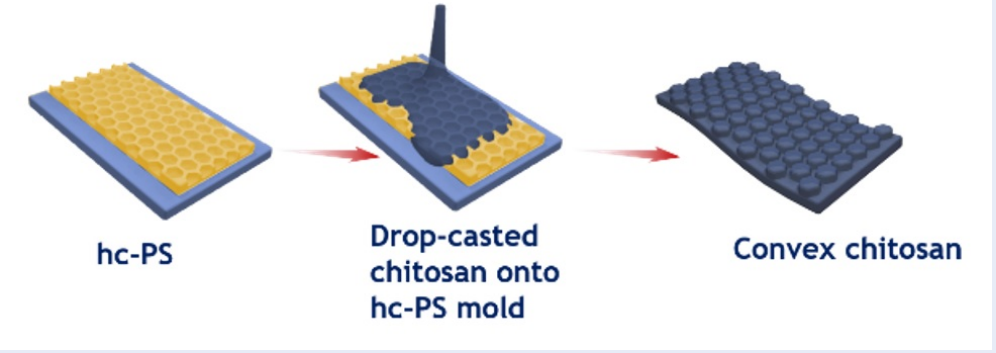

Figure 1: Scheme representing the fabrication of the chitosan film with microdome-patterned array.

Characterization

The characterization of samples' surface morphology was performed using the field-emission scanning electron microscopy (FE-SEM, S-4800, Hitachi, Japan). The static water contact angle (WCA) was evaluated by using a drop shape analyzer (Phoenix 300T, Seo, Korea). A custom-made pushing tester with feasibly of controlling ambient temperature and humidity was employed to trigger mechanical impulse to the TENG. The electrical output of TENG was measured by using a digital oscilloscope (SDS1102CML, Siglent, China) and an in-lab-made circuit as a current preamplifier [17].

RESULT AND DISSCUSION

Morphology of PI membranes

The porous PI films were obtained through one-step scalable solution immersion method, and the porosity of the membrane was controlled by adjusting polymer concentration. Three sponge-like PI membranes, which were prepared with PI content of 5 wt. %, 8 wt. %, and 10 wt. %, denoted as *p*-PI5, *p*-PI8; *p*-PI10, respectively. To provide more insight into the influence of polymer concentration on the formation of the porous structure, the scanning electron microscope (SEM) images and optical photographs of the porous PI films were characterized, as shown in Figure 3 (a-f). In general, along with the decrease in the polymer concentration, the porosity increased, thus the highest porosity was obtained with the *p*-PI5. In addition, the uniformity of the membrane surface is the best with *p*-PI8 and became lower with the *p*-PI5 and the *p*-PI10. This is mainly attributed to the viscosity of the polymer solution, which significantly influences the formation of the porous structure through the phase separation process. It is well-known that the viscosity increases with an increase in polymer concentration. Hence, the polymer concentration directly affects the morphological structure of the films as well as other film's parameters including the thickness and uniformity [18].

Particularly, with the low viscous polymer solution, the formation rate of porous structure was fast due to the solvent/nonsolvent pair easily diffused during the phase separation process, resulting in high porosity membrane and continuous sponge-like structure at the PI concentration of 5 wt. %, which can be seen in Figure 3b. In contrast, with the increasing solid content to 10 wt. %, *p*-PI10 membrane exhibited a skin layer on the top surface as highlighted in Figure 3f. This phenomenon not only decreases the pore size and porosity on the materials surface, but also creates a low uniformity region on the material surface, which was displayed in Figure 3e. For the application in a TENG, this region may result in poor contact between the two frictional surfaces. Meanwhile, at 8 wt. % of PI concentration, the membrane displayed not only bicontinuous sponge-like porous structure (Figure 3d) but also a good uniformity in a large scale, which was presented in the optical photograph (Figure 3c).

The polymer concentration also has a great effect on the film thickness regarding the solution immersion process. Accordingly, the thickness of PI membranes significantly increases from approximately 9 μm to 35 μm with the increase in PI content from 5 to 10 wt. % (Figure 4a). When the thickness of the triboelectric layer increases, more triboelectric charges can be built up and retained inside the porous structure. However, after the thickness reaches a certain value, the electrostatic induction between charges on the surface and the electrode becomes weaker, resulting in the decrease of the output of the TENG. In addition, wettability of the electrets was reported to greatly affect

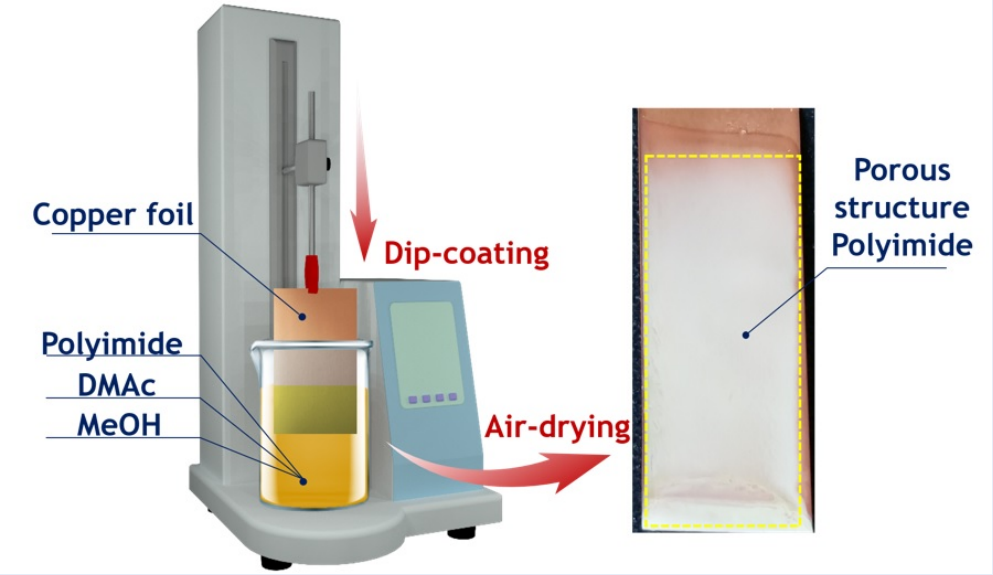

Figure 2: Schematic illustration of the one-step process for preparing the porous PI based on the evaporation-induced phase separation method.

the stability of TENG in humid environments. The comparison of the WCA values between commercial Kapton film and porous PI films with different polymer concentrations was shown in Figure 4b. Overall, the WCA of Kapton film with a flat surface was about 68°, WCA records the highest value at 116.7° of *p*-PI5 due to the significant increase in surface roughness. With the decrease of porosity, the WCA of *p*-PI8 and *p*-PI10 reduce to 98° and 59°, respectively. However, the *p*-PI8 is still presented as a hydrophobic surface due to its large porosity and uniform structure while the *p*-PI10 film becomes a hydrophilic surface similar to the commercial Kapton film due to the existence of a skin layer on the surface.

The thermal resistance of the porous PI and Celgard 2400 membranes was also evaluated by a thermal shrinkage test, in which the samples were heated in an oven at 200 °C for 30 min. It can be observed in Figure 5b that the Celgard 2400 membrane exhibited a vigorously shrink, combined with the color change from white (Figure 5a) to transparent. In other words, the Celgard 2400 membrane completely melted and the porous structure disappeared. In contrast, there was no obviously dimensional shrink and color change in the PI membrane. This result also indicated that the porous structure of PI membrane still remained until the temperature reached 200 °C. Therefore, the porous PI membrane would be a promising negative tribo-material to be applied in high temperature resistant TENG.

Output performance of the PI-TENG

To evaluate the electrical output performance of the porous PI-based TENG, the device with top standard Al electrode and bottom PI-Cu foil electrode was fabricated (Figure 6a). The current signal generated in a single working cycle of the TENG (Figure 6c) illustrated the its working principle. Before contacting, there is no charge generated on both PI and Al surfaces. When PI is contacted with an Al electrode, the friction between two tribo-materials occurs, and electrons are moved from Al to the PI membrane, resulting in positive and negative charges on both surfaces according to the triboelectric effect. Then, two surfaces are being separated, the negative charges on the PI porous surface induce positive charges on the Cu electrode. The established potential difference between Al and Cu electrodes creates an electron flow from the Al electrode to the Cu electrode through an external circuit, generating a negative current signal. When the two surfaces move closer again, electrons flow back from the top Al electrode to the Cu electrode due to the electrostatic field, until the system goes back to the fully pressed equilibrium state (Figure 6b).

For comparison, the open-circuit voltage (V_{OC}) of the nanogenerator devices using different types of PI structures (commercial Kapton and flat PI) with the same test conditions were shown in Figure 6d. As expected, the TENG with *p*-PI8 reached the highest

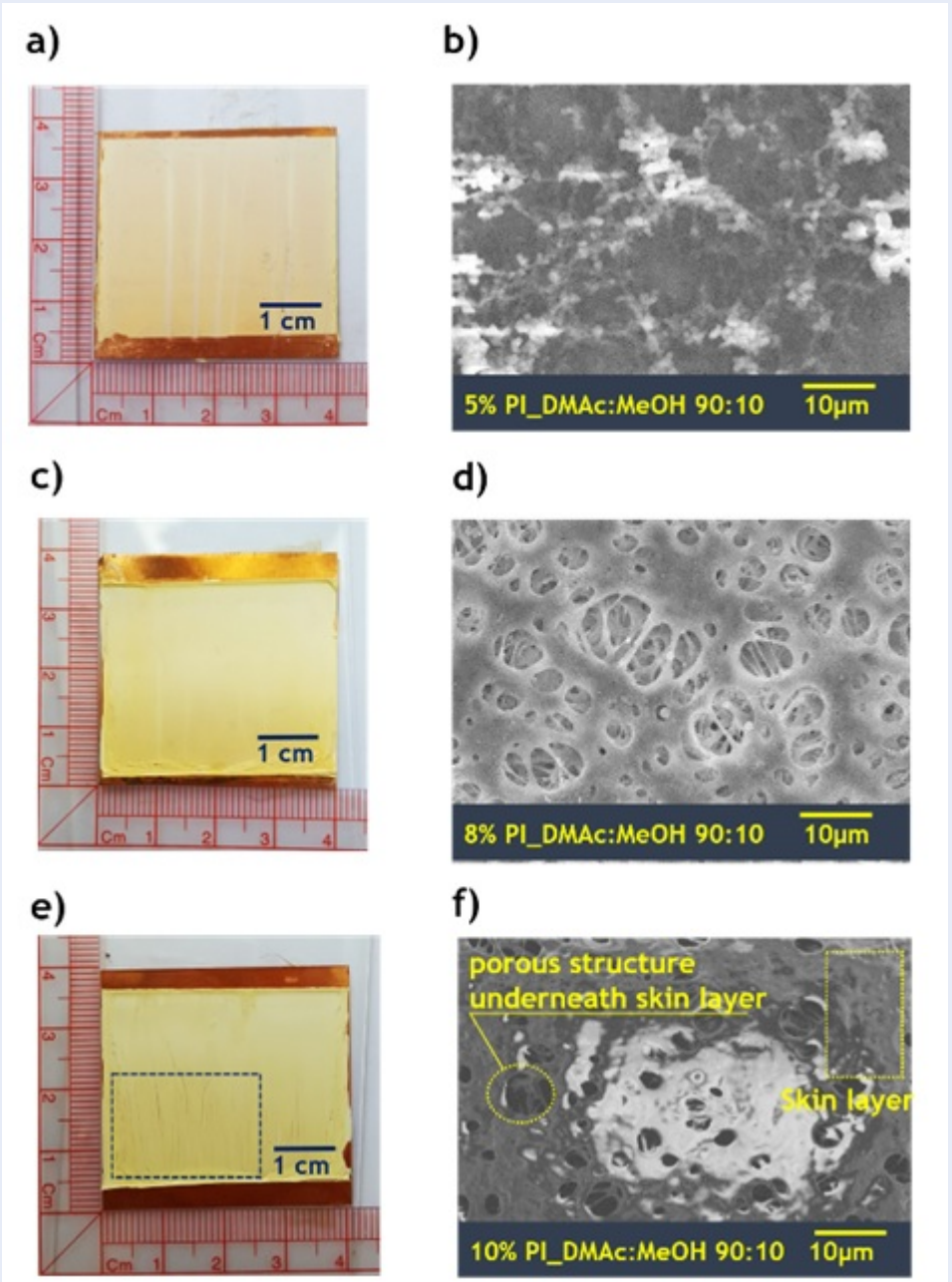

Figure 3: (a-f) Optical photographs and SEM images of porous PI films prepared with different polymer concentrations.

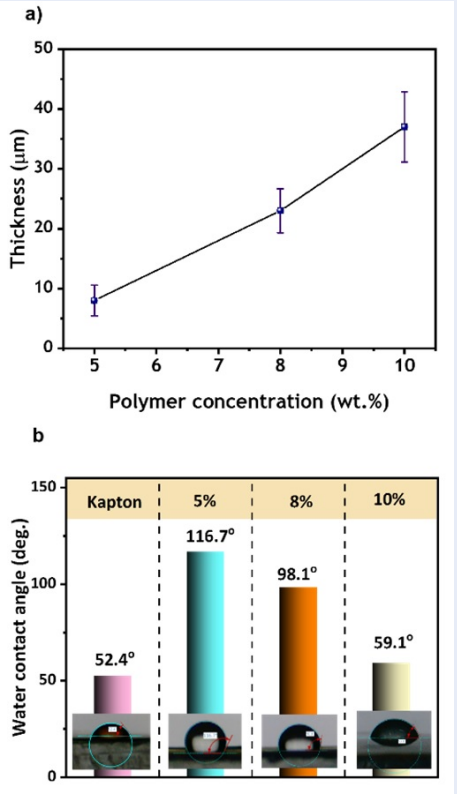

Figure 4: a) Change of the thickness of the PI membranes corresponding to polymer concentration of the solutions. b) Water contact angle (WCA) of the Kapton and the porous PI films.

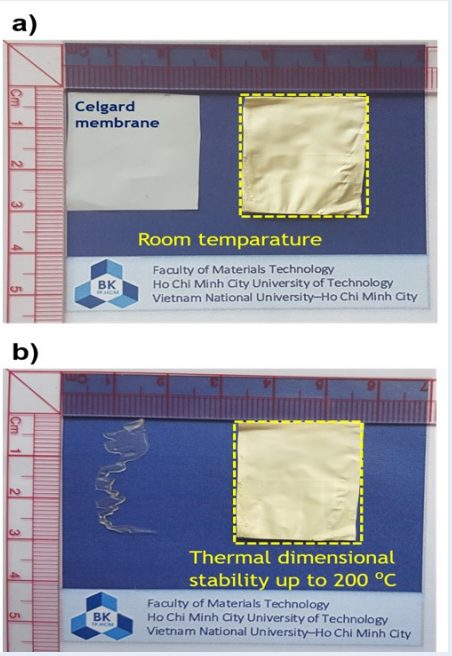

Figure 5: Photographs of *p*-PI8 and the Celgard 2400 membranes before and after thermal shrinkage test.

V_{OC} of approximately 40 V. Obviously, V_{OC} of *p*-PI8-based TENG is much higher than that of the TENGs using either the Kapton or the flat PI with the V_{OC} of 17 V and 4 V, respectively. This improvement can be explained due to the large surface area of the *p*-PI8 surface compared with the planar dense PI, leading to an enhancement of the electrification effect.

To evaluate the output power generation of the PI-based TENG, various external loads with different resistance values was used. As present in Figure 6e, the VOC increased gradually when the resistance was increased in the range of $10^6 \div 10^8$ Ω. Using these results, the dependence of the instantaneous power density generated from the PI-based TENG on the loads was calculated ($P = \frac{U^2}{R}$). The instantaneous power density of the PI-TENG reached a maximum value of about 0.049 mW/cm^2 at a matched resistance of 4×10^6 Ω. Additionally, the instantaneous output powers of the PI-TENG under different frequencies were investigated with the results presented in Figure 6f. As expected, the output power slightly increased with increasing the triggering frequency from 1 to 5 Hz.

For demonstration of potential practical applications, the porous PI and chitosan with uniformly microdome patterned surface were also fabricated (Figure 7a). The output voltage of PI/chitosan TENG obtained a value of over 180 V under a 5-Hz frequency, which was as high as 4.5 times compared with PI/Al-based TENG (Figure 7b). The enhancement of power generation capability of the PI-TENG is attributed to enhancement of both electrification effectiveness and electrostatic induction. The better matching between the concave-porous PI and convex-patterned chitosan counterpart leads to a great increase in effectively frictional area. Furthermore, the choice of tribomaterials is also a determining factor in the power output of TENGs. The greater differences in electron affinity of the two selected contact materials, the better electrical output performance. Due to this, chitosan as one of the best candidates for the positive tribomaterial and PI as the most negative tribo-material were combined to become an ideal friction layer pair for our new TENG. As shown in Figure 7c, a 1 μF-capacitor can be quickly charged to over 2.5 V within 50 s by the TENG, then used as a power supply to power electronic devices. In addition, Figure 7(d-e) showed the "HCMUT" panel with 102 light-emitting

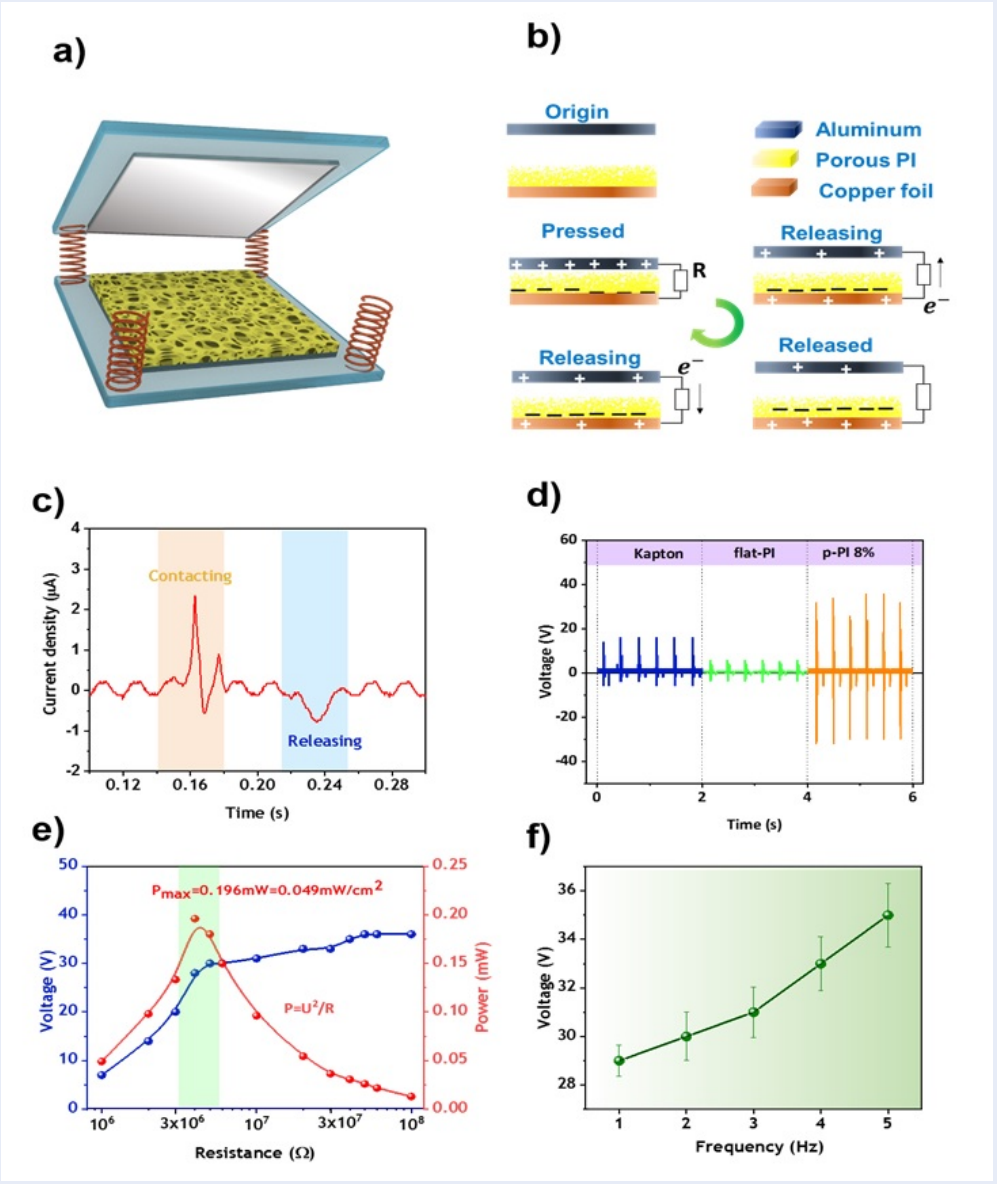

Figure 6: Characterization of electrical output and working principle of the PI-TENG: (a) 3D sketch representing the structural design of the PI-TENG with two frictional surfaces of porous PI and aluminum; (b) Working mechanism of the PI-TENG (c) Electrical current signal generated on a single working cycle of the TENG; (d) Open-circuit voltage (V_{oc}) of the nangenerator devices using different PI surfaces; (e) Instantaneous power of the PI-TENG at different load resistances; (f) The effect of triggering frequency on the output voltage.

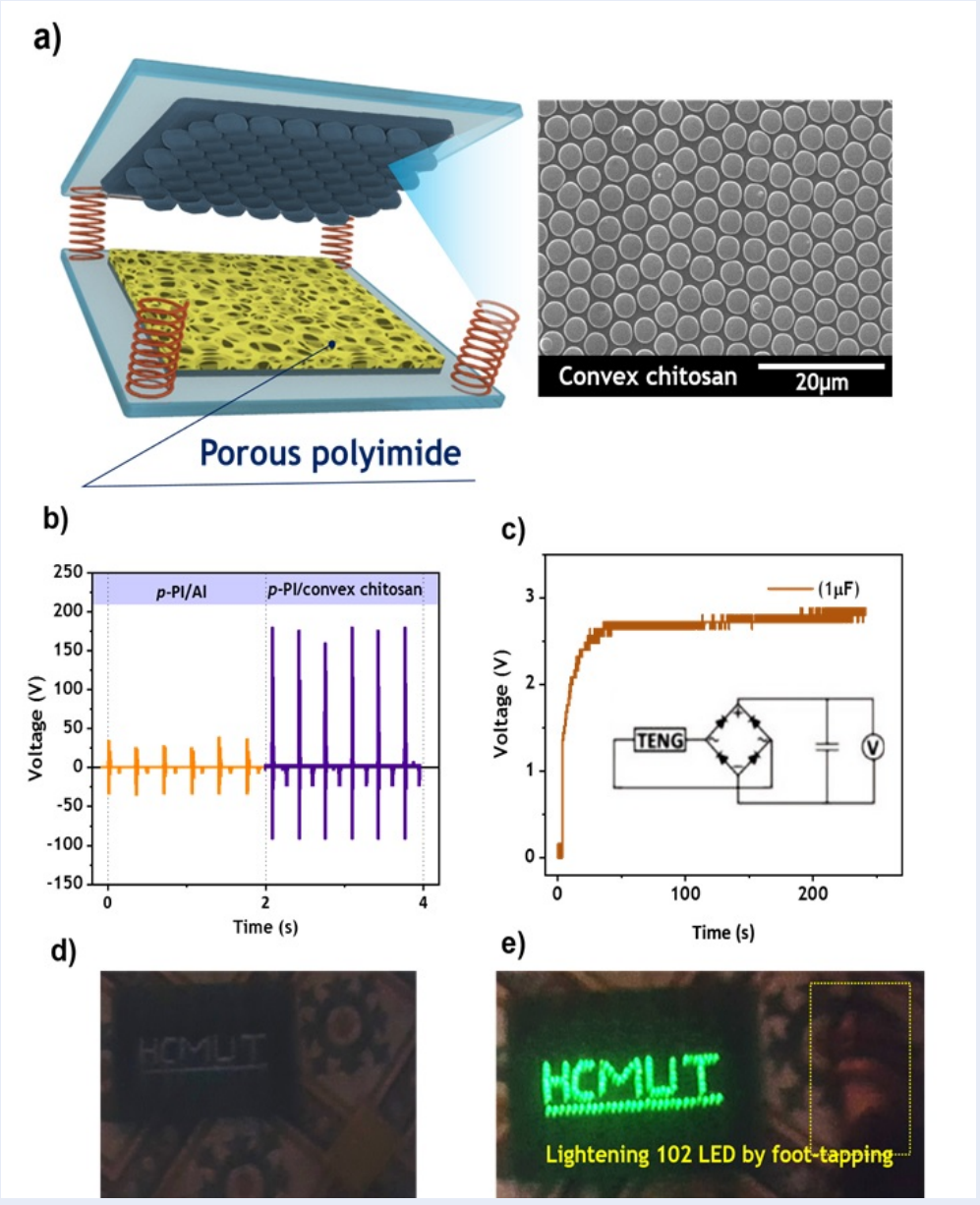

Figure 7: (a) 3D Sketch of the TENG device assembled with porous PI and convex-patterned chitosan. (b) SEM image of surface of the patterned Chitosan. (c) Open-circuit voltage (V_{oc}) of TENG devices using Al and patterned chitosan surfaces. (d) Charging curve of a 1 F-capacitor for the porous PI-based TENG device. (e) PI-based TENG device used to harvest mechanical energy from footsteps for instantly lighting on 400 blue LEDs.

diodes (LEDs) before and after being lightened simply by foot-tapping the TENG.

CONCLUSION

In this work, polyimide films with high porosity were successfully fabricated via an one-step scalable solution immersion method. A 8 wt. % PI solution in a mixture of DMAc and methanol with DMAc/methanol ratio of 90/10 was found to be a suitable condition for the fabrication of the uniformly porous structure. In addition, the porous PI exhibited excellent thermal stability without obviously thermal shrinkage even after being heated up to 200 °C. The TENG device assembled with the porous PI and aluminum possessed an output voltage of 40 V, which is 10 times higher than TENG using flat PI. Moreover, by combining with a microdome-patterned chitosan as a counter antagonistically structured surface, the TENG showed about 4.5 times enhancement in output voltage compared to the one using Al surface. We believe that the present porous PI-based TENG can be utilized in various harsh-environment applications such as separators for high-temperature batteries, supercapacitors, fuel cells, and actuators.

ACKNOWLEDGEMENT

This research is funded by The Murata Science Foundation. We acknowledge Ho Chi Minh City University of Technology (HCMUT), VNU-HCM for supporting this study.

LIST OF ABBREVIATIONS

DMAc Dimethyl Acetamide
hc-PS Honeycomb Polystyrene
IPS Improved Phase Separation
ISC Short-Circuit Current
MeOH Methanol
PI Polyimide
PMMA Poly(methyl methacrylate)
SEM Scanning Electron Microscope
TENG Triboelectric NanogeneratorVOC Open-Circuit Voltage
WCA Water Contact Angle

COMPETING INTERESTS

The authors declare no competing financial interest.

AUTHOR CONTRIBUTIONS

Thu Ha Le: Conceptualization, Investigation, Discussion;
Ngoc Mai Chau: Investigation;
Thi Le Thanh Nguyen: Discussion;
Van-Tien Bui: Supervision, Funding acquisition, Resources, Writing –Reviewing and Editing.

REFERENCES

1. Lund H. Renewable energy strategies for sustainable development. Energy. 2007;32(6):912-9;Available from: https://doi.org/10.1016/j.energy.2006.10.017.
2. Li H, Lv S, Fang Y, Micro B-I. Bio-inspired micro/nanostructures for flexible and stretchable electronics. Nano Res. 2020;13(5):1244-52;Available from: https://doi.org/10.1007/s12274-020-2628-9.
3. Shi Q, He T, Lee C. More than energy harvesting - combining triboelectric nanogenerator and flexible electronics technology for enabling novel micro-/nano-systems. Nano Energy. 2019;57:851-71;Available from: https://doi.org/10.1016/j.nanoen.2019.01.002.
4. Fan FR, Tian ZQ, Lin Wang Z. Flexible triboelectric generator. Nano Energy. 2012;1(2):328-34;Available from: https://doi.org/10.1016/j.nanoen.2012.01.004.
5. Kwak SS, Yoon HJ, Kim SW. Textile-based triboelectric nanogenerators for self-powered wearable electronics. Adv Funct Mater. 2019;29(2):1-26;Available from: https://doi.org/10.1002/adfm.201804533.
6. Chen A, Zhang C, Zhu G, Wang ZL. Polymer materials for high-performance triboelectric nanogenerators. Adv Sci (Weinh). 2020;7(14):2000186;PMID: 32714748. Available from: https://doi.org/10.1002/advs.202000186.
7. Bian Yaoxing, Jiang T, Xiao Tianxiao, Gong W, Cao X, Wang Zhaona et al. Triboelectric nanogenerator tree for harvesting wind energy and illuminating in subway tunnel. Adv Mater Technol. 2018;3(3):1700317;Available from: https://doi.org/10.1002/admt.201700317.
8. Zhao Z, Pu X, Du C, Li L, Jiang C, Hu W et al. Freestanding flag-type triboelectric nanogenerator for harvesting high-altitude wind energy from arbitrary directions. ACS Nano. 2016;10(2):1780-7;PMID: 26738695. Available from: https://doi.org/10.1021/acsnano.5b07157.
9. Liu Y, Zheng Y, Wu Z, Zhang L, Sun W, Li T et al. Conductive elastic sponge-based triboelectric nanogenerator (TENG) for effective random mechanical energy harvesting and ammonia sensing. Nano Energy. 2021;79:105422;Available from: https://doi.org/10.1016/j.nanoen.2020.105422.
10. Xu Z, Zhang D *, Haolin Cai , Yan Yang , Hao Zhang, C. Du. Performance Enhancement of Triboelectric Nanogenerators Using Contact-Separation Mode in Conjunction with the Sliding Mode and Multifunctional Application for Motion Monitoring. Nano Energy 2022, 102, 107719;Available from: https://doi.org/10.1016/j.nanoen.2022.107719.
11. Chen J, Ren Y, Xiang H, Jiang X, Yang X, Guo H. A self-powered human-pet interaction system enabled by triboelectric nanogenerator functionalized pet-leash. Nano Energy. 2022;101:107597;Available from: https://doi.org/10.1016/j.nanoen.2022.107597.
12. Saadatnia Z, Mosanenzadeh SG, Esmailzadeh E, Naguib HE. A high performance triboelectric nanogenerator using porous polyimide aerogel film. Sci Rep. 2019;9(1):1370;PMID: 30718775. Available from: https://doi.org/10.1038/s41598-018-38121-1.
13. Mi HY, Jing X, Meador MAB, Guo H, Turng LS, Gong S. Triboelectric nanogenerators made of porous polyamide nanofiber mats and polyimide aerogel film: output optimization and performance in circuits. ACS Appl Mater Interfaces. 2018;10(36):30596-606;PMID: 30114352. Available from: https://doi.org/10.1021/acsami.8b08098.
14. Zhang Y, Ionov L. Actuating porous polyimide films. ACS Appl Mater Interfaces. 2014;6(13):10072-7;PMID: 24903283. Available from: https://doi.org/10.1021/am502492u.
15. Li Z, Zou H, Liu P. Morphology and properties of porous polyimide films prepared through thermally induced phase separation. RSC Adv. 2015;5(47):37837-42;Available from: https://doi.org/10.1039/C5RA01514F.

16. Bui VT, Ko SH, Choi HS. A surfactant-free bio-compatible film with a highly ordered honeycomb pattern fabricated via an improved phase separation method. Chem Commun (Camb). 2014;50(29):3817-9;PMID: 24592398. Available from: https://doi.org/10.1039/c3cc48654k.
17. Mallineni SSK, Behlow H, Podila R, Rao AM, Low-Cost A. A low-cost Approach for measuring electrical load currents in triboelectric nanogenerators. Nanotechnol Rev. 2018;7(2):149-56;Available from: https://doi.org/10.1515/ntrev-2017-0178.
18. Yang T-I, Su T-L, Lin P, Tseng I, Chang C, Fang H. , 5Fabrication of porous polylactic acid films assisted by dip-coating and template leaching techniques. J Appl Polym Sci. 2012;124(3):2333-9;Available from: https://doi.org/10.1002/app.35277.

Tạp chí Phát triển Khoa học và Công nghệ – Engineering and Technology, 5(S1):109-119

Open Access Full Text Article

Chế tạo màng polyimide cấu trúc xốp liên tục bằng phương pháp phân pha có kiểm soát từ hệ dung dịch ba cấu tử ứng dụng cho máy phát điện nano chịu nhiệt

Lê Thu Hà[1,2], Châu Ngọc Mai[1,2], Nguyễn Thị Lê Thanh[1,2], Bùi Văn Tiến[1,2,*]

Use your smartphone to scan this QR code and download this article

TÓM TẮT

Máy phát điện ma sát nano (TENG) là công nghệ thu hồi chuyển hóa năng lượng xanh mới đang thu hút được nhiều sự quan tâm của các nhóm nghiên cứu trên thế giới do TENG có thể được ứng dụng trong nhiều các lĩnh vực khác nhau. Một trong các ứng dụng quan trọng của TENG là nguồn cung cấp điện cho các cảm biến di động, các thiết bị điện tử đeo được công suất nhỏ. Tuy nhiên, vật liệu ma sát dùng trong chế tạo TENG thường là polymer, loại vật liệu thường bị suy giảm tính chất ở nhiệt độ cao. Điều này gây trở ngại cho TENG sử dụng trong các thiết bị cần phải hoạt động ở môi trường khắc nghiệt. Trong nghiên cứu này, chúng tôi đề xuất phương pháp chế tạo màng xốp polyimide (PI) chịu nhiệt độ cao bằng phương pháp một giai đoạn dựa trên quá trình phân pha được gây ra bởi quá trình bay hơi dung môi. Hỗn hợp N, N-dimethylacetamide và methanol được sử dụng là cặp dung môi/phi dung phù hợp để thực hiện quá trình tách pha hình thành cấu trúc xốp. Kết quả thu được cho thấy màng PI sở hữu cấu trúc xốp đồng đều với độ xốp lớn trên toàn bộ mẫu, đặc biệt, cả năng chịu nhiệt tuyệt vời của màng còn được so sánh với màng xốp Celgard thương mại. Thiết bị TENG sử dụng màng xốp PI đã chế tạo được ghép với bề mặt tích điện dương là nhôm có khả năng tạo ra điện thế 40 V, tương ứng gấp 10 và 2 lần so với màng PI không có cấu trúc xốp và màng Kapton. Đặc biệt, TENG thiết kế sử dụng bề mặt ma sát có cấu trúc đối nghịch gồm màng lồi chitosan và màng xốp PI có thể tạo ra điện thế 180 V, trực tiếp thắp sáng 102 đèn LED thương mại. Từ những ưu điểm như cho điện thế cao ổn định, chịu nhiệt độ cao và dễ chế tạo ở quy mô lớn, thiết bị TENG được chế tạo có tiềm năng ứng dụng cao trong việc cấp nguồn cho các thiết bị điện tử làm việc ở môi trường khắc nghiệt.

Từ khoá: Phương pháp phân pha, cấu trúc xốp, xốp liên tục, polyimide, máy phát điện nano ma sát

[1]*Bộ môn Vật liệu Polyme, Khoa Công Nghệ Vật Liệu, Trường Đại học Bách Khoa, 268 Lý Thường Kiệt, Quận 10, TP. Hồ Chí Minh, Việt Nam*

[2]*Đại học Quốc Gia TP. Hồ Chí Minh, Phường Linh Trung, TP. Hồ Chí Minh, Việt Nam*

Liên hệ

Bùi Văn Tiến, Bộ môn Vật liệu Polyme, Khoa Công Nghệ Vật Liệu, Trường Đại học Bách Khoa, 268 Lý Thường Kiệt, Quận 10, TP. Hồ Chí Minh, Việt Nam

Đại học Quốc Gia TP. Hồ Chí Minh, Phường Linh Trung, TP. Hồ Chí Minh, Việt Nam

Email: tienbv@hcmut.edu.vn

Lịch sử

- Ngày nhận: 25-04-2022
- Ngày chấp nhận: 31-01-2023
- Ngày đăng: 15-2-2023

DOI : https://doi.org/10.32508/stdjet.v5iSI1.990

Check for updates

VNUHCM PRESS

Trích dẫn bài báo này: Hà L T, Mai C N, Thanh N T L, Tiến B V. **Chế tạo màng polyimide cấu trúc xốp liên tục bằng phương pháp phân pha có kiểm soát từ hệ dung dịch ba cấu tử ứng dụng cho máy phát điện nano chịu nhiệt**. *Sci. Tech. Dev. J. - Eng. Tech.;* 5(S1):109-119.